Applied Nanoscience (2021) 11:199–206
https://doi.org/10.1007/s13204-020-01571-z

ORIGINAL ARTICLE

Fabrication of p–n heterojunction Ag_2O@Ce_2O nanocomposites make enables to improve photocatalytic activity under visible light

N. R. Khalid[1] · Amna Arshad[1] · M. B. Tahir[1] · M. Khalid Hussain[1]

Received: 2 August 2020 / Accepted: 25 September 2020 / Published online: 6 October 2020

Abstract

The design of highly efficient heterostructure material having good photocatalytic efficiency is good technique for the degradation of organic pollutants. In this paper, a series of Ag_2O/Ce_2O p–n heterostructure were prepared via facile hydrothermal approach with varying concentration of Ag_2O to Ce_2O (0%, 2%, 4%, and 6%). The crystal structure, morphology, chemical composition, optical properties and photocatalytic activity of synthesized nanostructures were studied. All test verified the development of p–n heterostructure which has reduced band gap energy as well as lower recombination of charge carriers. Moreover, this novel p–n heterojunction showed excellent charge carrier separation and transfer ability, thus superior photocatalytic efficiency under visible photo-illumination towards the degradation of methyl orange dye. Among all samples. 4% Ag_2O/Ce_2O nanocomposite exhibited superior photocatalytic activity, which is greatly higher than pure Ag_2O, Ce_2O and other nanocomposites. These results indicate that the synthesized p–n heterojunction will provide significant advancement in environmental field.

Keywords Ag_2o/ce_2O · Nanorods · p–n heterojunction · Optical properties · MO degradation

Introduction

The waste of the major industries as a whole consists of dyes that are organic in nature but non-biodegradable and toxic (Amini et al. 2011). These non-degradable dyes are the basic source of water pollution (Ong et al. 2014). There are many techniques available for water purification and sanitization that are widely used all over the world like filtration with membrane (Chidambaram et al. 2015) and oxidation in electrochemical process (Pirilä et al. 2015). Among all these techniques, the simplest and economically feasible technique is photocatalytic process (Azat and Gaukhar 2018; Konsowa et al. 2010). In this process, the catalyst is used in the presence of light to degrade the contaminants of water (Saravanakumar et al. (2016)). Many semiconductor including TiO_2, ZnO and Ce_2O etc. were used for photocatalytic process. (Wei et al. 2018; Kwong et al. 2007; Ahmad et al. 2013; Alammar and Mudring 2009; Xie et al. 2014; Akbari-Fakhrabadi et al. 2015; Khalid et al. 2019a). Among these, the Ce_2O has gained a lot of interest due to its low cost and good optical and photocatalytic properties (Amanulla et al. 2018; Wang et al. 2011a; Ranjith et al. 2018). It is highly stable chemically like TiO_2 and has band gap between 2.8–3.2 eV (Krishna Chandar and Jayavel 2013; Rohini et al. 2017). Therefore, it has the ability to absorb ultraviolet light efficiently. However, its absorbance of visible light is very low due to wider band gap (Ansari and Khan 2014). Recently, some researchers have focused on nanostructured ceria to improve its optical and photocatalytic properties. Different studies demonstrated that nanostructured ceria is more effective than bulk ceria in terms of its photocatalytic performance (Ghori and Veziroglu 2018). Moreover, it was also observed that doping of noble metals and their combination have showed good photoelectric response of nanostructured ceria under visible light irradiations (Durmus et al. 2019). The analysis of the earlier reported research revealed that the doping or combination of noble metal oxides has significantly enhanced degradation rate of the pollutants present in the contaminated water (Mathew et al. 2020; Li et al. 2020). The intrinsic properties of Ce_2O-based materials could be further modified by fabricating cerium oxide particles on nanoscale level as described earlier (Sayyed et al. 2016; Munoz-Batista et al. 2015). The

✉ M. B. Tahir
m.bilaltahir@uog.edu.pk

[1] Department of Physics, University of Gujrat, Hafiz Hayat Campus, Gujrat 50700, Pakistan

synthesis methods also play vital role in modifying the properties of nanostructured materials. However, some methods are complex and use toxic chemicals. Therefore, there are only few preparation methods which can provide controlled morphology and good properties (Saravanan et al. 2013). The synthesis of Ce_2O nanoparticles at higher temperature using conservative solid-state reaction pathway results in poor chemical activity and high impurity concentration with bulky particle size. Hydrothermal technique for the fabrication of nanoparticles in the form of aqueous solutions potentially provides an easy route that allows controlled morphology and the desired properties of the synthesized Ce_2O nanoparticles.

In addition to above, the coupling of pure Ce_2O with less band gap semiconductor (Ag_2O) is also an active technique to boost its efficiency as photocatalyst (Wen et al. 2018a). Ag_2O has 1.2 eV band gap energy and is also p type semiconductor due to which it can absorb visible light effectively (Yang et al. 2016; Chu et al. 2016; Wang et al. 2011b; Yu et al. 2016). However, alone Ag_2O photocatalyst has lower performance due to poor stability and short life time of electron–hole pairs. Therefore, formation of Ag_2O-based p–n heterojunction is very effective technique to enhance its photocatalytic performance as well as photogenerated charge carrier's life time (Khalid et al. 2019b; Wang et al. 2012; Ivanova et al. 2018; Wen et al. 2018b). Recently, Wen et al. (Wen et al. 2018b) have prepared novel Ag_2O/Ce_2O heterojunction photocatalyst by thermal decomposition process and applied for the degradation enrofloxacin. They observed that the formed heterojunction between Ag_2O and Ce_2O is good strategy to enhance charge carrier serration as well as good photocatalytic activity. However, complete understanding of Ag_2O/Ce_2O-based p–n heterojunction is still lacking and needs further study.

Here, we have applied simple hydrothermal process for the synthesis of Ag_2O/Ce_2O-based p–n heterostructure by varying the concentrations of Ag_2O. The loading of Ag_2O into Ag_2O/Ce_2O nanocomposite had reduced Ce_2O band gap and inhibited the electron–hole recombination. Moreover, the prepared Ag_2O/Ce_2O-based nanocomposites showed excellent photocatalytic efficiency for discoloring of methyl orange under visible photo-illumination.

Experimental

Synthesis of pure Ce_2O and Ag_2O/Ce_2O nanocomposite

Pure ceria and Ag_2O coupled Ag_2O/Ce_2O nanocomposites were synthesized via simple hydrothermal technique. Firstly, 2 g cerium nitrate ($Ce(NO_3)_3$) and required amount of silver nitrate was mixed in 10 ml deionized water to prepare the required solution under magnetic stirring of 15 min. In the second step, 13 g of sodium hydroxide NaOH was mixed into 70 ml deionized water to make another solution. For obtaining homogeneous solution, both above mentioned solutions were mixed under continuous magnetic stirring of 30 min. The mixture immediately after stirring was put into autoclave (Teflon-lined stainless-steel) having 100 mL volume, sealed tightly and thermally treated in temperature-controlled oven at 180 °C for 6 h. After hydrothermal treatment, the solution was thoroughly washed using deionized water for six time and dried at 100 °C for 10 h in an oven. Then obtained powder was calcined at 550 °C for 3 h in a muffle-furnace. The loading concentration of Ag_2O into Ag_2O/Ce_2O nanocomposite was controlled to be 0, 2, 4 and 6 wt%.

Characterization

Crystal size and structure of all prepared samples were investigated by XRD (JCPDS Card No:65-6811) having CuKα source with $\lambda = 0.1541$ nm. Scanning electron microscopy (SEM) was carried out on JEOL JSM-6330F to analyze the morphology of synthesized nanocomposites. The UV–visible spectrometer (Shimadzu UV–visible 1800) was utilized to study the optical absorption properties of photocatalysts. XPS analysis was carried out for chemical composition by Thermo ESCALAB 250 with Al K_α X-ray. The JASCO FP-8200 fluorescence-spectrophotometer was used with excitation wavelength of 350 nm for photoluminescence (PL) properties.

Photocatalytic performance testing

The all prepared photocatalyst were used to discolor the methyl orange dye dissolved in aqueous solution using irradiation of visible-light ($\lambda \geq 420$ nm). The solution for photocatalytic reaction was prepared via mixing 10 mg photocatalyst into the 100 ml aqueous solution that contains the 10 mg/ methyl orange dye. Before exposure of visible-light, the solution was kept in dark for 30 min under magnetic stirring to obtain equilibrium of absorption & desorption. Then the mixture was irradiated with visible light to proceed the photocatalytic process. After each interval of 30 min, sample was collected to determine the dye degraded concentration using UV–visible spectrometer.

Results and discussion

XRD analysis

The structural characteristics of the prepared Ce_2O, Ag_2O and Ag_2O/Ce_2O nanocomposite were examined through

the XRD pattern analysis as displayed in Fig. 1. The pure Ce_2O XRD patterns indicated the sharp intensity peaks at angle (2θ) of 28.20°, 33.32°, 47.11°,55.48°, 59.19°, 69.21°,76.71° and 79.06° with the planes (1 1 1), (2 0 0), (2 2 0), (3 1 1), (2 2 2), (4 0 0), (3 3 1) and (4 2 0) respectively. It was noted that the all peaks belong to cubic ceria phase according to JCPDS Card No: 43-1002. On the other hand, the sharp peaks of pure Ag_2O were obtained at 2θ values of 26.74°,32.5°, 38.5°, 54.9°, 65.71° and 68.91° can be indexed to (1 1 0), (1 1 1), (2 0 0), (2 2 0), (3 3 1) and (2 2 2) confirmation the face centered cubic structure of Ag_2O (JCPDS, Card No.65-6811). XRD patterns of Ag_2O coupled Ce_2O (Ag_2O/Ce_2O) nanocomposites demonstrate that the there is no major difference between pure Ce_2O and Ag_2O/Ce_2O composite samples. However, intensity of peaks was decreased after increasing the ratio of Ag_2O. Secondly, Ce_2O peak at 33.32° 2θ angle was shifted toward lower angle. It could be attributed to the reason that the main observed peak of Ag_2O at 32.5° is close to 33.32° peak of Ce_2O which might be overlapped in nanocomposite samples. The results show that Ag_2O/Ce_2O nanocomposites were formed and incorporation of silver oxide did not severely affect the crystalline structure of cerium oxide. Moreover, Scherer's equation was utilized to determine the crystallite size of all synthesized nanostructures using XRD patterns by the following formula (Alammar and Mudring 2009): wherever k is a factor of shape, λ is X-rays wavelength, β represents the full width of half maximum and θ represents angle of peak respectively.

$$D = \frac{k\lambda}{\beta \cos\theta} \quad (1)$$

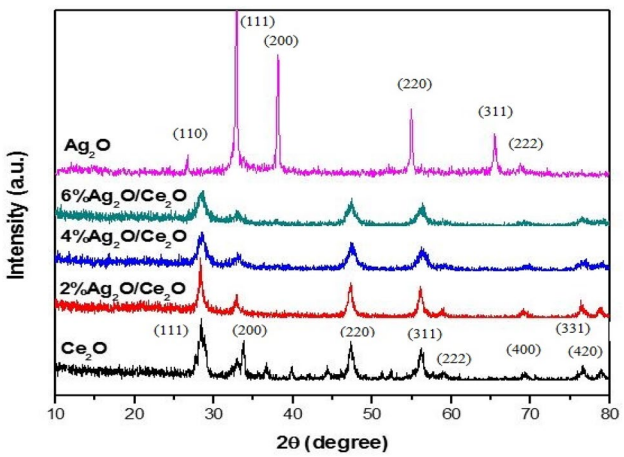

Fig. 1 XRD crystal structures of Ce_2O, Ag_2O and Ag_2O/Ce_2O nanocomposites

The calculated average crystallite sizes were 12 nm, 20 nm, 11 nm, 10.2 nm, 9.8 nm for Ce_2O, Ag_2O, $2Ag_2O/Ce_2O$, $4Ag_2O/Ce_2O$ and $6Ag_2O/Ce_2O$, respectively. This shows that Ag_2O loading into Ag_2O/Ce_2O nanocomposite has decreased the crystallite size of samples which again confirms the formation development of Ag_2O/Ce_2O nanostructure.

SEM analysis

Surface morphology of 4% Ag_2O/Ce_2O nanostructure was inspected with scanning electron microscopy. Figure 2 demonstrates the SEM images of nanocomposite at varying resolutions. The images clearly reveal nanorods like morphology of composite sample. These nanorods have average length of ~ 2 µm and diameter ~ 0.15 µm. This novel morphology prepared through hydrothermal process confirms that our prepared sample has greater surface area, surface active sights and thus will act as excellent photocatalytic material.

XPS Analysis

The chemical states of $4Ag_2O/Ce_2O$ nanostructure were examined via XPS and spectra are displayed in Fig. 3. In Ce 3d core level spectrum (Fig. 3a), four peaks are detected, the first two peaks at 906 eV and 902.2 are due to Ce $3d_{3/2}$ and the other two peaks at 888.6 eV and 885.4 eV are due to Ce $3d_{5/2}$. These peaks clearly indicate Ce^{4+} chemical state of cerium in Ag_2O/Ce_2O nanocomposite (Wen et al. 2018b; Xu and Wang 2012). The Fig. 3(b) displays XPS highly resolved Ag 3d spectrum, it has two peaks at binding energies of 374.5 and 368.5 eV which could be ascribed to Ag $3d_{3/2}$ and Ag $3d_{5/2}$ of Ag + (Wen et al. 2018b, 2017). In O 1 s core spectrum two peaks are present (Fig. 3c), the first peak at 532 eV is due to adsorbed oxygen and H_2O and the second appearing at 530.0 eV can be attributed to Ag–O and Ce–O bonds (Wen et al. 2018b).

UV–visible analysis

The optical absorption properties of pure Ce_2O and $4Ag_2O/Ce_2O$ nanocomposite was studied using UV–visible spectroscopy. As displayed in Fig. 4a, pure Ce_2O exhibits absorption edge at 421 nm wavelength in visible-light region. After the loading of Ag_2O into Ag_2O/Ce_2O composite, absorption edge is shifted towards higher wavelength at about 445 nm. The energy band gap (E_g) of both samples were determined using Tauc plot equation (Khalid et al. 2019b); where h ν denotes photon energy of incident light, α is known as absorption coefficient, A is known as proportionality constant and E_g is energy band gap. Band gap energy was

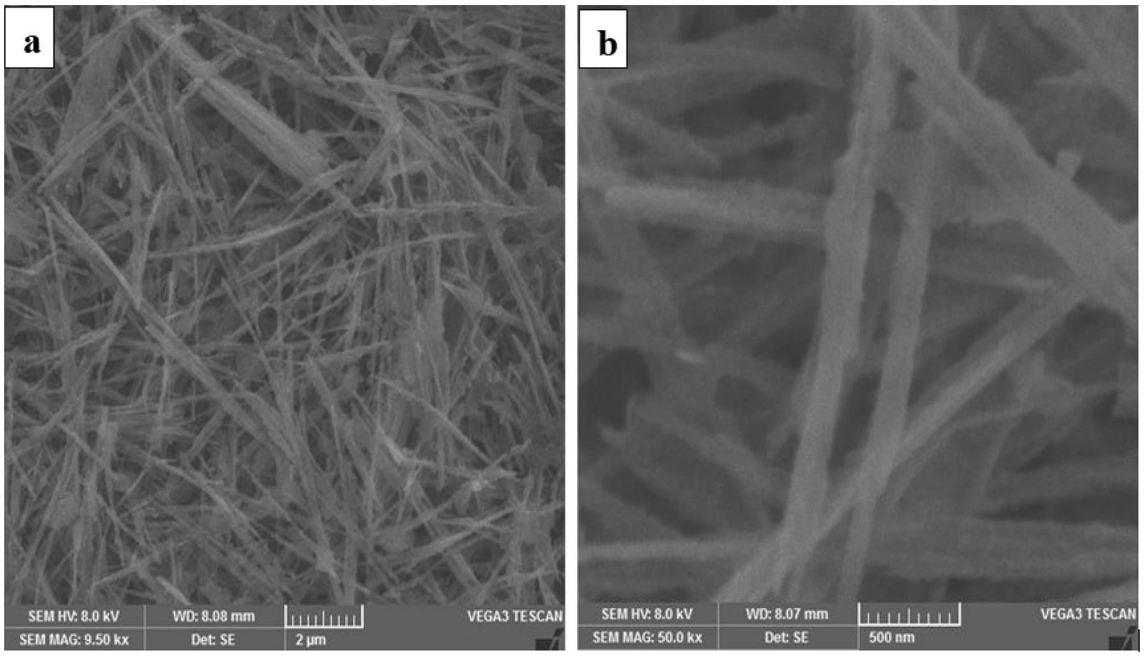

Fig. 2 SEM image of the Ag_2O/Ce2O composite at different concentrations of temperature and time

founded by plotting graph between $(\alpha h\ \nu)^2$ versus $(h\ \nu)$ using spectral data of Fig. 4a and results are displayed in Fig. 4b:

$$(\alpha h\nu)^2 = A\ (h\nu - E_g). \quad (2)$$

Thus, band gap (E_g) of pure Ce_2O and $4Ag_2O/Ce_2O$ nanocomposite was found to be 2.94 nm and 2.79 nm, respectively. These finding confirms that Ag_2O incorporation has the ability to reduce the band gap of cerium oxide.

PL analysis

The photoluminescence (PL)spectroscopy has gained greater attention in photocatalysis to study the surface processes in which photoexcited electrons and holes participate (Wen et al. 2018b; Swain et al. 2017). Moreover, PL emission represents the photocreated charge carrier's recombination. The higher PL emission intensity represents greater electron–hole recombination. Therefore, in order to explore the effect of Ag_2O loading onto Ag_2O/Ce_2O nanocomposites, PL spectra were measured for pure Ag_2O, Ce_2O and Ag_2O/Ce_2O nanocomposites and results are displayed in Fig. 5. The spectra demonstrate that the bare Ag_2O and Ce_2O exhibited higher PL emission intensity indicating greater recombination of electrons and holes. However, with the incorporation of Ag_2O into Ag_2O/Ce_2O nanocomposite the PL emission intensity was decreased. It could be observed that among all samples, $4Ag_2O/Ce_2O$ nanocomposite showed lowest PL emission intensity confirming the inhibition of electrons and holes recombination. Therefore, it is expected that this nanocomposite with optimum loading of Ag_2O (4%) will perform excellently for discoloration of dye during photocatalysis.

Photocatalytic degradation activity

The photocatalytic efficiencies of as-prepared photocatalysts were inspected by degradation of methyl orange (MO) dye under visible photo-irradiation. The dye (MO) adsorption on catalysts surface in the dark for 30 min and photocatalytic performance results are displayed in Fig. 6. It was seen that $4Ag_2O/Ce_2O$ nanocomposite showed maximum adsorption than all other samples. It could be attributed to nanorods like morphology of nanocomposite. Furthermore, photocatalytic activity results show that nanocomposites had degraded the dye more effectively than pure Ce_2O and Ag_2O photocatalysts. Interestingly, it can be seen that with increasing ratio of Ag_2O into Ag_2O/Ce_2O nanocomposite upto 4%, the photocatalytic performance was increased. This shows that loading ratio of Ag_2O has significant role to improve photocatalytic efficiency of photocatalyst. It can be ascribed to the fact that optimum loading ratio may develop more active surface sites on photocatalysts which would increase its efficiency. However, further increase in Ag_2O incorporation (6%) had decreased the performance of nanocomposite due to aggregation of Ag_2O particles onto the photocatalyst surface which resulted into lower efficiency of photocatalyst.

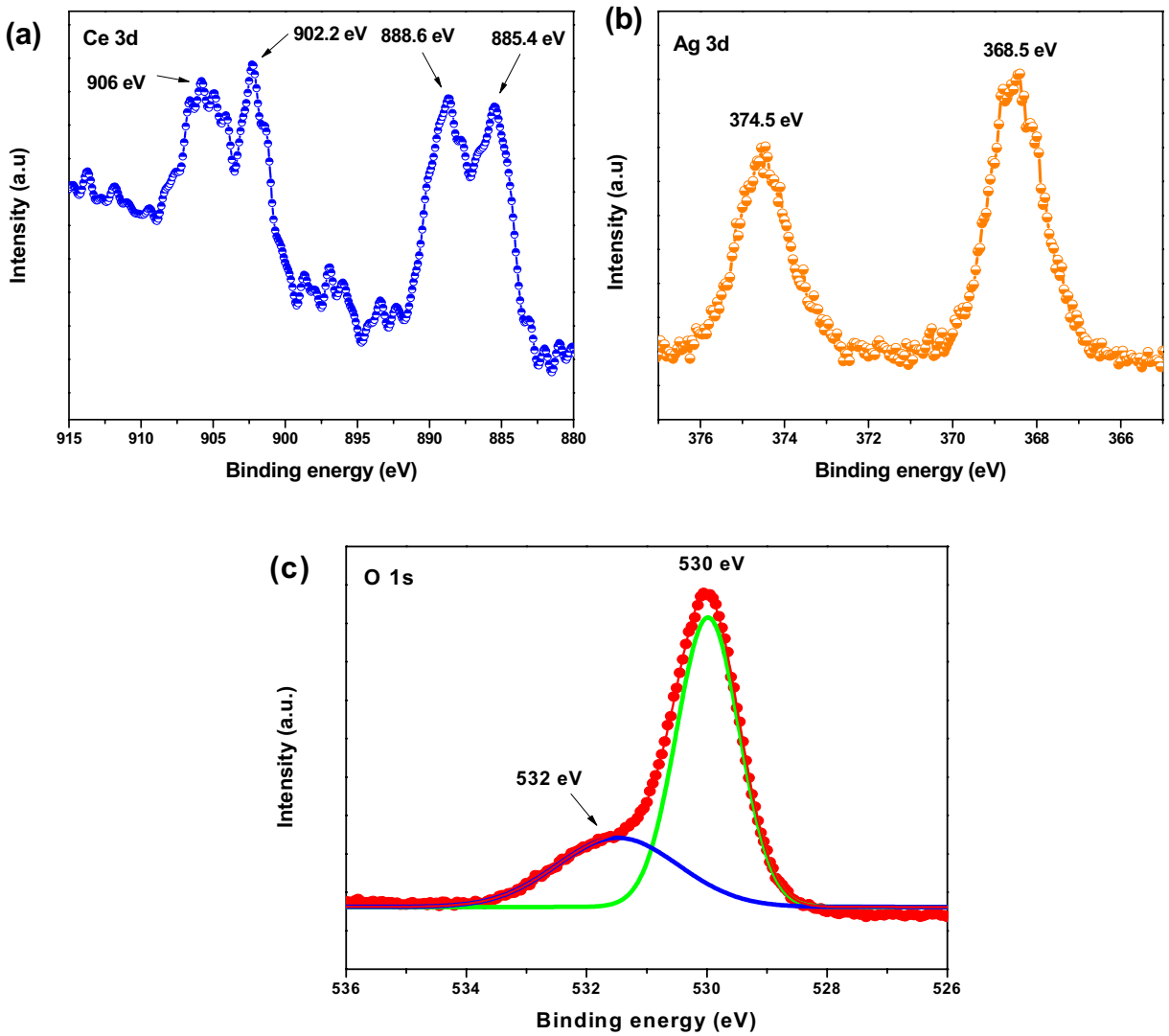

Fig. 3 XPS core level spectra (**a**) Ce 3d, **b** Ag 3d, **c** O 1 s of 4%Ag_2O/Ce_2O nanocomposite

Photocatalytic degradation mechanism

The relative band positions of both semiconductors were found to understand the improved photocatalytic activity of Ag_2O/Ce_2O nanocomposite. It is generally known that band-edge potential levels play an important role in determining the transfer of photocreated electrons and holes in heterostructure nanocomposites. Therefore, valence band (VB) tops for both semiconductors were calculated according to following equation (Swain et al. 2017); where X and E_g are the electronegativity and semiconductor band gap energy and E_0 represents free electron energy on hydrogen scale (~4.5).

$$E_{CB} = E_{VB} - E_g \tag{3}$$

The values of electronegativity (X) for Ce_2O and Ag_2O were calculated to be 5.578 and 5.29 respectively. The energy band gap value of Ce_2O was used 2.94 eV from Fig. 4 and band gap energy of Ag_2O was used 1.3 eV according to previous reports (Akel et al. 2018). The calculated valence band tops for Ce_2O and Ag_2O were 2.58 and 1.44 respectively.

The conduction band (CB) bottoms of Ce_2O and Ag_2O were determined from following equation (Swain et al. 2017);

$$E_{CB} = E_{VB} - E_g \tag{4}$$

The calculated conduction band bottoms of Ce_2O and Ag_2O were −0.36 and +0.14 respectively. Based on above calculations, a photocatalysis mechanism of Ag_2O/Ce_2O heterostructure is proposed in Fig. 7. Upon exposure of visible light, both

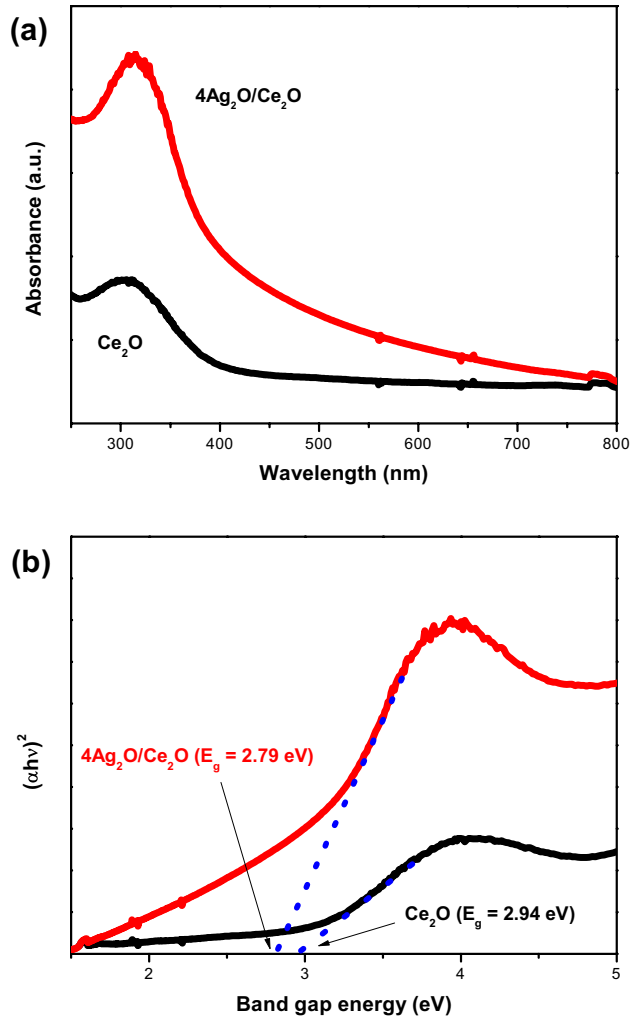

Fig. 4 **a** UV–visible absorption spectra (**b**) Tauc plot of Ce_2O and 4% Ag_2O/Ce_2O nanocomposite

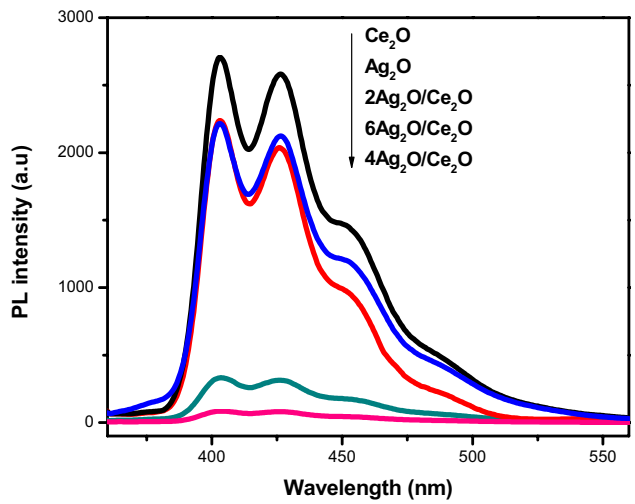

Fig. 5 PL spectra of different samples

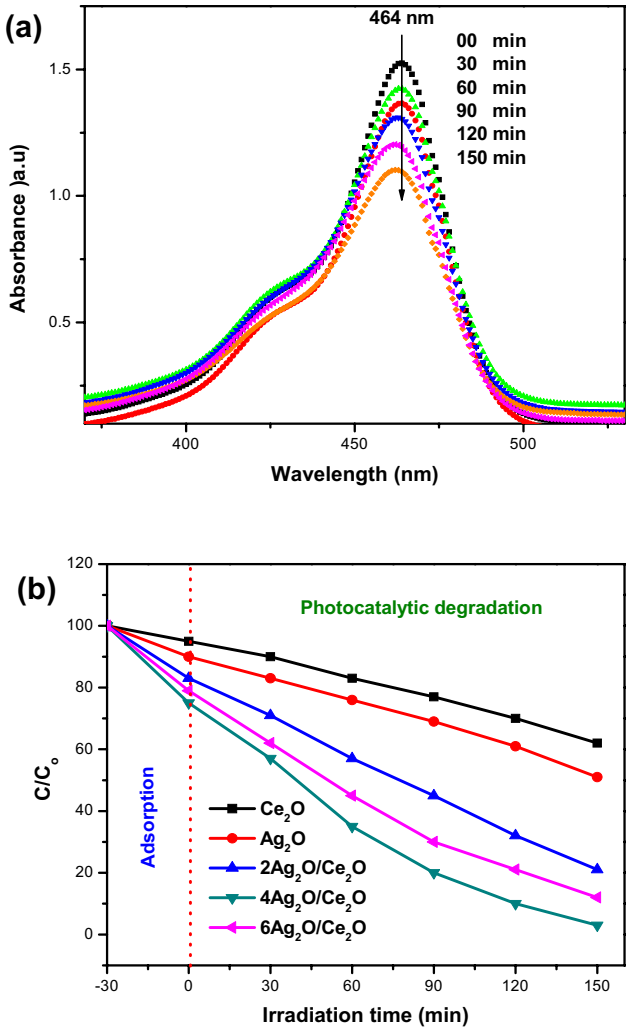

Fig. 6 **a** UV–visible absorption spectra of methyl orange (MO) dye degradation using 4% Ag_2O/Ce_2O nanocomposite, **b** Photocatalytic degradation performance of different photocatalysts for MO under visible light irradiation ($\lambda \geq 420$ nm)

semiconductors Ce_2O and Ag_2O create holes in valence band and electrons in conduction band. Due to more positive potential of valence band of Ce_2O (2.58) than that of Ag_2O (1.44), the photocreated holes in valence band of Ce_2O could transfer to valence band Ag_2O. At the same time, electrons will be transferred from conduction band of Ce2O toward conduction band of Ag_2O because Ce_2O has more negative conduction band potential of conduction band as compare to conduction band potential of Ag_2O.

Conclusion

In the present research, a facile hydrothermal technique is adopted for the synthesis of Ag_2O/Ce_2O nanorod-based photocatalysts. The obtained Ag_2O/Ce_2O nanocomposites

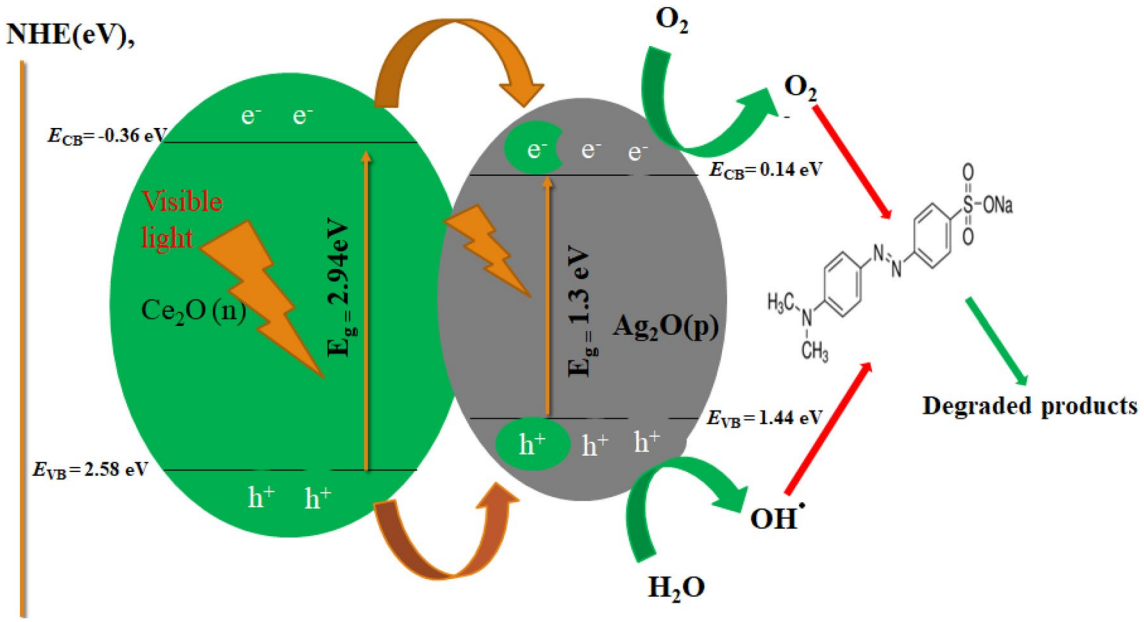

Fig. 7 Schematic diagram of proposed reaction mechanism for MO dye degradation using % Ag_2O/Ce_2O nanocomposite

exhibited superior photocatalytic performance for methyl orange dye degradation under visible photoillumination**.** The improved photocatalytic efficiency was ascribed to novel morphology, reduced band gap of nanocomposite and inhibited recombination of electrons and holes due to formed heterojunction between Ag_2O and Ce_2O. This study could offer a new methodology to fabricate a novel p–n heterojunction photocatalyst for advanced photocatalysis in energy and environmental field.

Compliance with ethical standards

Conflict of interest No potential conflict of interest was reported by the authors.

References

Amini M, Arami M, Mahmoodi NM et al (2011) Dye removal from colored textile wastewater using acrylic grafted nanomembrane. Desalination 267:107–113

Ong YK, Li FY, Sun SP et al (2014) Nanofiltration hollow fibre membranes for textile wastewater treatment: lab-scale and pilot-scale studies. Chem Engin Sci 114:51–57

Chidambaram T, Oren Y, Noel M (2015) Fouling of nanofiltration membranes by dyes during brine recovery from textile dye bath wastewater. Chem Engin J 262:156–168

Pirilä M, Saouabe M, Ojala S et al (2015) Photocatalytic degradation of organic pollutants in wastewater. Top Catal 58:1085–1099

Azat Y, Gaukhar B et al (2018) Photocatalytic treatment of a synthetic wastewater. Mater Sci Engin 301:012143

Konsowa AH, Ossman ME, Chen Y, Crittenden JC (2010) Decolorization of industrial wastewater by ozonation followed by adsorption on activated carbon. J Hazard Mater 176:181–185

Saravanakumar K, Ramjan MM, Suresh P et al (2016) Fabrication of highly efficient visible light driven Ag/Ce_2O photocatalyst for degradation of organic pollutants. J Alloys Comp 664:149–160

Wei X, Rui L, Qingyu X (2018) Enhanced photocatalytic activity of Se-doped TiO_2 under visible light irradiation. Sci Rep 8:8752

Kwong HL, Yeung HL, Yeung CT et al (2007) Chiral pyridine-containing ligands in asymmetric catalysis. Coordination Chem Rev 251:2188–2222

Ahmad M, Ahmed E, Zhang Y et al (2013) Preparation of highly efficient Al-doped ZnO photocatalyst by combustion synthesis. Curr Appl Phys 13:697–704

Alammar T, Mudring AV (2009) Facile preparation of Ag/ZnO nanoparticles via photoreduction. J Mater Sci 44:3218–3222

Xie CM, Lu X, Wang KF et al (2014) Silver nanoparticles and growth factors incorporated hydroxyapatite coatings on metallic implant surfaces for enhancement of osteoinductivity and antibacterial properties. ACS Appl Mater Interf 6:8580–8589

Akbari-Fakhrabadi A, Saravanan R, Jamshidijam M et al (2015) Preparation of nanosized yttrium doped Ce_2O catalyst used for photocatalytic application. J Saudi Chem Soci 19:505–510

Khalid NR, Hammad A, Tahir MB et al (2019a) Enhanced photocatalytic activity of Al and Fe co-doped ZnO nanorods for methylene blue degradation. Ceramics Int 45:21430–21435

Amanulla AM, Shahina SJ, Sundaram R et al (2018) Antibacterial, magnetic, optical and humidity sensor studies of β-$CoMoO_4$-Co_3O_4 nanocomposites and its synthesis and characterization. J Photochem Photobiol B 183:233–241

Wang X, Li S, Ma Y, Yu H, Yu J (2011a) $H_2WO_4{\cdot}H_2O$/Ag/AgCl composite nanoplates: a plasmonic Z-scheme visible-light photocatalyst. Phys Chem C 115:4648–14655

Ranjith KS, Dong CL, Lu YR et al (2018) Evolution of visible photocatalytic properties of Cu-doped Ce2O nanoparticles: role of Cu2+-mediated oxygen vacancies and the mixed-valence states of Ce ions. ACS Sustainable Chem Eng 6:8536–8546

Krishna Chandar N, Jayavel R (2013) C14TAB-assisted Ce_2O mesocrystals: self-assembly mechanism and its characterization. Appl Nanosci 3:263–269

Rohini BS, Nagabhushana H, Darshan GP et al (2017) Fabricated Ce_2O nanopowders as a novel sensing platform for advanced forensic, electrochemical and photocatalytic applications. Appl Nanosci 7:815–833

Ansari SA, Khan MM et al (2014) Band gap engineering of Ce_2O nanostructure using an electrochemically active biofilm for visible light applications. RSC Adv 4:6782–16791

Ghori MZ, Veziroglu S et al (2018) Role of UV plasmonics in the photocatalytic performance of TiO_2 decorated with aluminum nanoparticles. ACS Appl Nano Mater 1:3760–3764

Durmus Z, Kurt BZ, Durmus A (2019) Synthesis and characterization of graphene oxide/zinc oxide (Go/ZnO) nanocomposite and its utilization for photocatalytic degradation of basic fuchsin dye. Chem Select 4(1):271–278

Mathew S, Antony A, Kathyayini H (2020) Degradation of azo dye under visible light irradiation over nanographene oxide–zinc oxide nanocomposite as catalyst. Appl Nanosci 10:253–262

Li H, Gao M, Gao Q et al (2020) Palladium nanoparticles uniformly and firmly supported on hierarchical flower-like TiO_2 nanospheres as a highly active and reusable catalyst for detoxification of Cr(VI)-contaminated water. Appl Nanosci 10:359–369

Sayyed SAAR, Beedri NI, Kadam VS et al (2016) Rose Bengal sensitized bilayered photoanode of nano-crystalline TiO_2–Ce_2O for dye-sensitized solar cell application. Appl Nanosci 6:875–881

Munoz-Batista MJ, Fernández-García M, Kubacka A (2015) Promotion of Ce_2O–TiO_2 photoactivity by g-C_3N_4: ultraviolet and visible light elimination of toluene. Appl Catal B 164:261–320

Saravanan R, Karthikeyan S, Gupta VK, Sekaran G, Narayanan V, Stephen AJ (2013) Enhanced photocatalytic activity of ZnO/CuO nanocomposite for the degradation of textile dye on visible light illumination. Mater Sci Engin C 33:91–98

Wen XJ, Niu CG, Zhang L, Liang C, Zeng GM (2018a) A novel Ag_2O/Ce_2O heterojunction photocatalysts for photocatalytic degradation of enrofloxacin: possible degradation pathways, mineralization activity and an in depth mechanism insight. Appl Catal B Environ 221:701–714

Yang S, Xu D, Chen B, Luo B, Yan X, Xiao L, Shi W (2016) Synthesis and visible-light-driven photocatalytic activity of p-n heterojunction Ag_2O/$NaTaO_3$ nanocubes. Appl Surf Sci 383:214–221

Chu H, Liu X, Liu J, Li J, Wu T, Li H, Lei W, Xu Pan L (2016) Synergetic effect of Ag_2O as co-catalyst for enhanced photocatalytic degradation of phenol on N-TiO_2. Mater Sci Engin B 211:128–134

Wang X, Li S, Yu H, Yu J, Liu S (2011b) Ag_2O as a new visible-light photocatalyst: self-stability and high photocatalytic activity. Chem A European J 17:7777–7780

Yu H, Chen W, Wang X, XuY YuJ (2016) Enhanced photocatalytic activity and photoinduced stability of Ag-based photocatalysts: the synergistic action of amorphous-Ti(IV) and Fe(III) cocatalysts. App Catal B 163:163–170

Khalid NR, Hussain MK, Murtaza G, Ikram M, Ahmad M, Hammad A (2019b) A novel Ag_2O/Fe–TiO_2 photocatalyst for CO_2 conversion into methane under visible light. J Inorg Organomet Polym 29:1288–1296

Wang W, Jing L, Qu Y, Luan Y, Fu H, Xiao Y (2012) Facile fabrication of efficient AgBr-TiO_2 nanoheterostructured photocatalyst for degrading pollutants and its photogenerated charge transfer mechanism. J Hazard Mater 243:169–178

Ivanova TV, Homola T, Bryukvin A et al (2018) Catalytic performance of Ag_2O and Ag doped Ce_2O prepared by atomic layer deposition for diesel soot oxidation. Coatings 8:237

Wen XJ, Niu CJ, Zhang L et al (2018b) A novel Ag_2O/Ce_2O heterojunction photocatalysts for photocatalytic degradation of enrofloxacin: possible degradation pathways, mineralization activity and an in depth mechanism insight. Appl Catal B Environ 221:701–714

Xu L, Wang J (2012) Magnetic nanoscale Fe_3O_4/Ce_2O composite as an efficient Fenton-like heterogeneous catalyst for degradation of 4-chlorophenol. Environ Sci Technol 46:10145–10153

Wen XJ, Zhang C, Niu CJ et al (2017) Highly enhanced visible light photocatalytic activity of Ce_2O through fabricating a novel p-n junction BiOBr/Ce_2O. Catal Commun 90:51–55

Swain G, Sultana S, Naik B et al (2017) Coupling of crumpled-type novel MoS_2 with Ce_2O nanoparticles: a noble-metal-free p−n heterojunction composite for visible light photocatalytic H_2 production. ACS Omega 2:3745–3753

Akel S, Dillert R, Balayeva NO et al (2018) Ag/Ag_2O as a co-catalyst in TiO_2 photocatalysis: effect of the co-catalyst/photocatalyst mass ratio. Catalysts 8:647